

A Varactor Controlled Phase Shifter for PCS Base Station Applications



APN1009

Introduction

Power amplifiers in today's base stations use compensation techniques to reduce distortion. There are many well-known compensation techniques available, all relying on similar principles of phase and amplitude control. Thus, most (and possibly all) of the compensation techniques use the same control components: voltage-controlled attenuators and voltage-controlled phase shifters.

The quality of these control components strongly determines compensation circuit performance. The ideal phase shifter provides a linear (vs. voltage) 0–360° phase shift with 0 dB change in the signal level; similarly, the ideal attenuator would provide a linear (vs. voltage) attenuation change with 0° phase shift between attenuation settings.

This application note describes the design of a high performance phase shifter for PCS band base station applications. It employs the low cost Alpha SMV1245-011 varactor as the phase-control element and the Alpha HY19-12, 90° hybrid. The PCS band was selected because the large number of base stations employed in its infrastructure require an efficient, low cost solution. However, the methodology employed in this design is applicable to other wireless platforms.

Phase Shifter Fundamentals

A typical phase shifter architecture employing a quadrature coupler (90° hybrid) is shown in Figure 1. The input signal (P_{IN}) is divided by the coupler and directed to two branches (with 90° phase shift) that are terminated with varactor diodes D_1 and D_2 , changing the phase of each signal equally. The reflected signals ($P_{ref}/2$) are then re-combined and are in phase at the output port (P_{OUT}). The reflected signals at the input port are 180° out of phase and cancel each other. The phase shift provided by this circuit is equal to the reflection phase shift provided by a single varactor. The small vectors in Figure 1 show the phase relationships at the output and input ports.

A circulator terminated by a varactor may also be used to separate the reflected and incident waves and provide phase shift. However, this solution would be costly. Instead, the circuit in Figure 1 provides a lower cost alternative, although it uses two phase shifting varactor circuits.

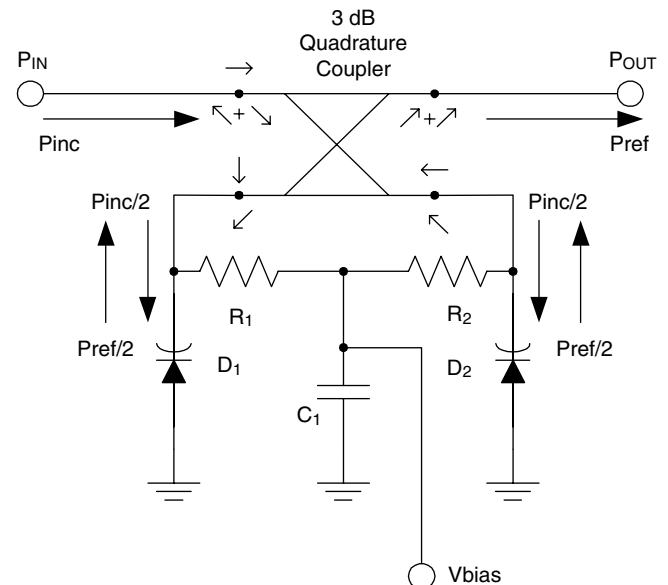


Figure 1. Typical Phase Shifter Design

The varactor components in Figure 1 act as ideal, lossless reactive loads with reflection coefficient from 0° (open circuit — zero varactor capacitance) to -180° (short circuit — infinite varactor capacitance). The reflection phase shift for different elementary circuits were calculated and are shown in Figure 2. For an ideal variable capacitor that changes from 0 pF to infinity, a total phase shift from 0° to -180° will occur. For an ideal variable inductor, the phase changes from -180° to 0°. If both were connected in series, the ideal result would be a 360° phase shift change.

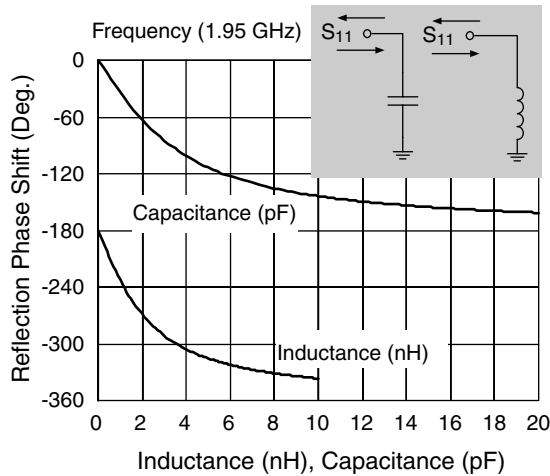


Figure 2a. Elementary L and C circuits

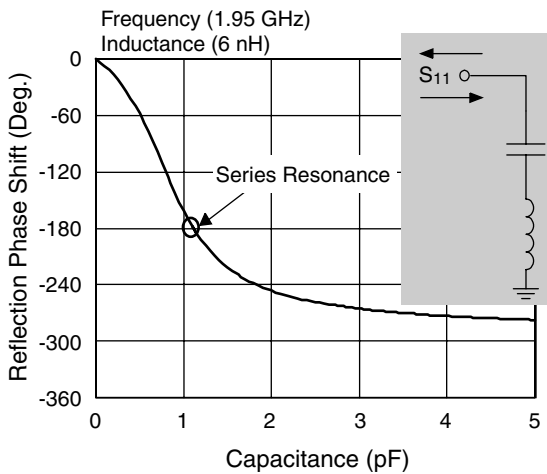


Figure 2b. Series LC Circuit

Figure 2a and 2b. Reflection (S_{11}) Phase Shift for Elementary Circuits

Figure 2b shows that adding a fixed inductor to a variable capacitor increases the phase shift range; in this case 6 nH was added at 1.95 GHz, resulting in a phase shift of approximately 280°. However, a continued increase of inductance will reduce the effect of the varactor capacitance range and lead to a degradation of the overall phase shift range. Installing an additional capacitor (C_{par}) in parallel with the LC varactor network, shown in Figure 3, reduces this effect.

The components shown in Figure 3 are used in a typical design. Two additional resistive components are included: the parasitic varactor series resistance (R_S) and the added

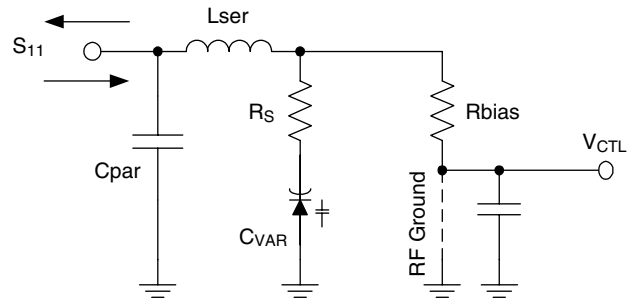


Figure 3. Equivalent Circuit of the Practical Phase Shifting Element

bias resistor (R_{bias}). Figure 4 shows the calculated loss, S_{11} , for different combinations of R_S and R_{bias} . The varactor R_S introduces most loss at maximum capacitance (highest current in varactor path). However, the bias resistance, in parallel with the varactor, introduces the highest loss at low capacitance, below the 180° phase shift point, where resonance occurs. From linear circuit theory, this resonance also depends on the value of R_{bias} . When these loss factors are taken into account, some flattening of the amplitude response may result, as shown in Figure 4.

In reality, the varactor resistance, R_S , may be a function of bias (reverse) voltage. In some “very” hyperabrupt junction varactors, the series resistance may vary 2–5 times from its maximum at 0 V to a minimum at the punch-through voltage. However, the series resistance of the SMV1245 used in this design is constant for the range of applied voltage.

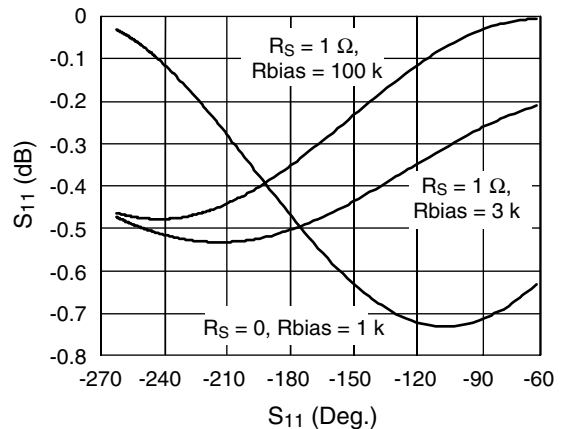


Figure 4. S_{11} State Chart for $C_{VAR} = 0-10$ pF (Ref. Fig. 3)

The Phase Shifter Circuit Model

The circuit model (for Libra IV) is shown in Figure 5. A quadrature hybrid (HYB1) is used with 0.6 dB loss, which effectively simulates the Alpha HY19-12 used in our design. Capacitors C₁ and C₂ are internal components within the HY19-12, which isolate the DC paths from input and output ports.

The 0.5 dB loss pad (PAD1) simulates the total loss of the input/output interface in the circuit board. In reality, the effect of the input/output interface, including SMA transitions and microstrip lines, is more complex than the pad used in the model. The simplification is appropriate

because the model concentrates on the phase and amplitude response vs. control voltage, which is not affected by the performance of the input/output interface.

Inductors L₁ and L₂ (both 0.9 nH) effectively simulate the HY19-12 lead and package inductances. Parallel capacitors SRLC1 and SRLC2 are simulated as a series R-L-C network with a package inductance of 0.75 nH and series resistance of 0.2 Ω. The discrete inductors SRL1 and SRL2 are modeled as lossy parallel R-L-C networks with series resistance, R_{lser} = 0.6 Ω, and parallel capacitance, 0.14 pF, which is typical for the majority of multilayer inductors with inductance values within 2–5 nH.

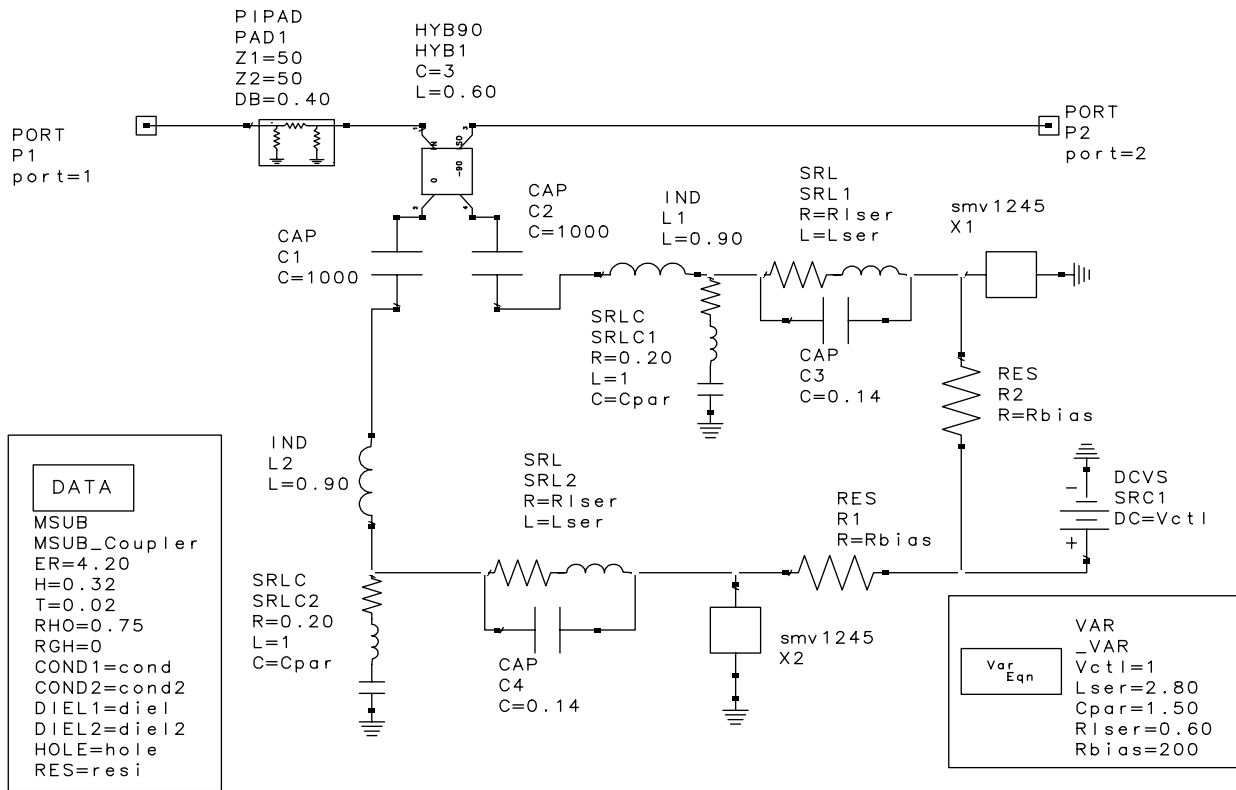


Figure 5. Phase Shifter Circuit Model

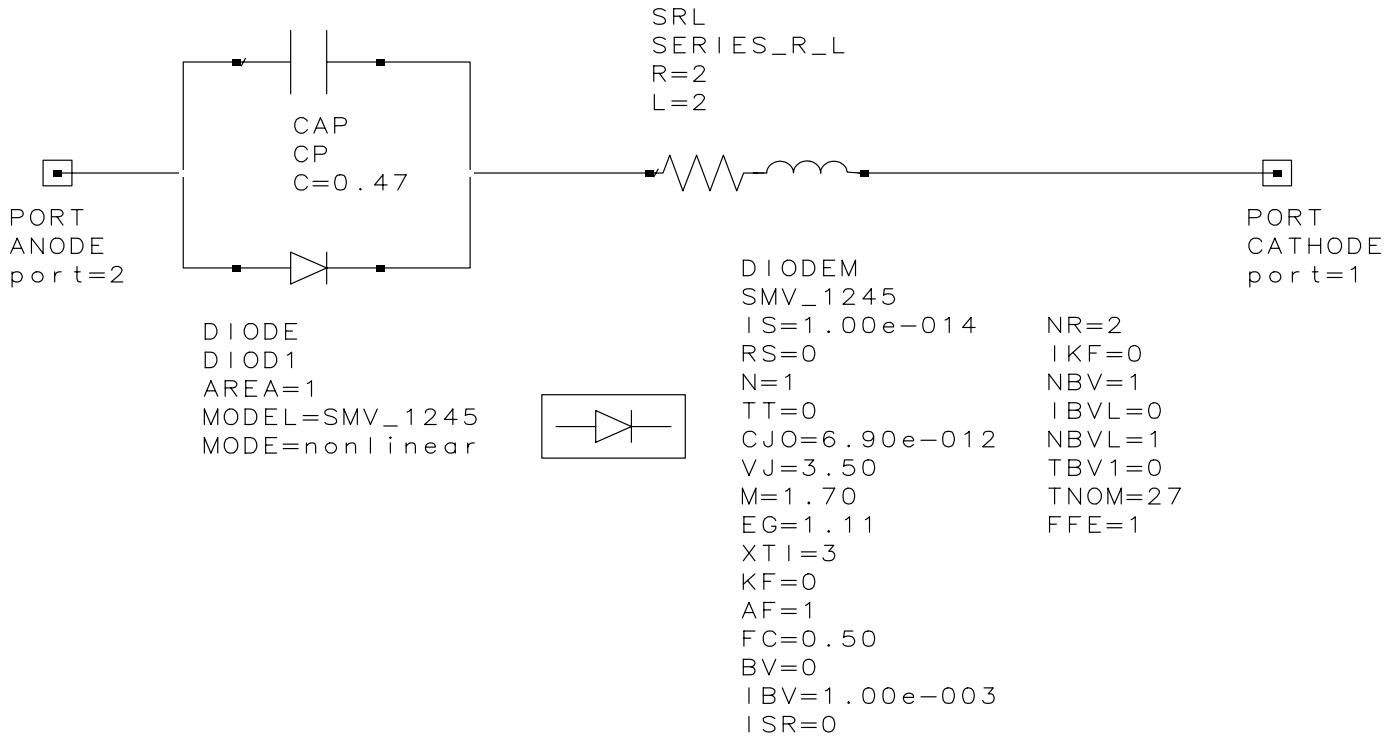


Figure 6. SMV1245 Spice Model

SMV1245-011 SPICE Model

The SMV1245-011 is a low capacitance hyperabrupt varactor diode in a SOD-323 package.

The SPICE model for the SMV1245-011 varactor diode, defined for the Libra IV environment, is shown in Figure 4 with a description of the parameters employed.

Table 1 describes the model parameters. It displays default values appropriate for silicon varactor diodes that may be used by the Libra IV (or similar) simulator.

According to the SPICE model, the varactor capacitance, C_V , is a function of the applied reverse DC voltage, V_R , and may be expressed as follows:

$$C_V = \frac{C_{JO}}{\left(1 + \frac{V_R}{V_J}\right)^M} + C_P$$

This equation is a mathematical expression of the capacitance characteristic. The model is most accurate for abrupt junction varactors (like Alpha’s SMV1408). However, for hyperabrupt junction varactors, the model is less accurate because the coefficients are dependent on the applied voltage. To improve the equation for hyperabrupt junction varactors, the coefficients were optimized for the best capacitance vs. voltage fit. These simulated coefficients may not have physical meaning.

SPICE model values for the capacitance, C_V , of SMV1245-011 used in the phase shifter design are given in Table 2.

Note that in the Libra model, C_P , is given in pico-Farads, while C_{GO} is given in Farads to comply with the default unit system used in Libra.

Parameter	Description	Unit	Default SMP1320
IS	Saturation current (with N, determine the DC characteristics of the diode)	A	1e-14
R _S	Series resistance	Ω	0
N	Emission coefficient (with IS, determines the DC characteristics of the diode)	-	1
TT	Transit time	S	0
C _{JO}	Zero-bias junction capacitance (with V _J and M define nonlinear junction capacitance of the diode)	F	0
V _J	Junction potential (with V _J and M define nonlinear junction capacitance of the diode)	V	1
M	Grading coefficient (with V _J and M define nonlinear junction capacitance of the diode)	-	0.5
E _G	Energy gap (with XTI, helps define the dependence of IS on temperature)	EV	1.11
XTI	Saturation current temperature exponent (with E _G , helps define the dependence of IS on temperature)	-	3
KF	Flicker noise coefficient	-	0
AF	Flicker noise exponent	-	1
FC	Forward-bias depletion capacitance coefficient	-	0.5
B _V	Reverse breakdown voltage	V	Infinity
I _{BV}	Current at reverse breakdown voltage	A	1e-3
ISR	Recombination current parameter	A	0
NR	Emission coefficient for ISR	-	2
IKF	High-injection knee current	A	Infinity
NBV	Reverse breakdown ideality factor	-	1
I _{BVL}	Low-level reverse breakdown knee current	A	0
NBVL	Low-level reverse breakdown ideality factor	-	1
T _{NOM}	Nominal ambient temperature at which these model parameters were derived	°C	27
FFE	Flicker noise frequency exponent	-	1

Table 1. Silicon Diode Default Values in Libra IV

Part Number	C _{JO} (pF)	M	V _J (V)	C _P (pF)	R _S (Ω)	L _S (nH)
SMV1245-011	6.9	1.7	3.5	0.47	2	2

Table 2. SPICE Parameters for SMV1245-011

Phase Shifter Design, Materials and Layout

The circuit diagram for the phase shifter is shown in Figure 7 and the PC board layout is shown in Figure 8. A bill of materials for the phase shifter is shown in Table 3.

The PC board is made of 0.5 mm thick, standard FR4 material with two-sided copper (0.02 mm thick) metallization. For test purposes, the RF signals were fed through SMA connectors.

The 90° hybrid coupler is Alpha model HY19-12, a GaAs IC, optimized for PCS band applications. Although it is GaAs based, this product is passive and does not require external bias. All RF leads of the HY19-12 are DC isolated, minimizing the number of added DC blocking capacitors. Sufficient grounding is provided through the four VIA holes under the IC body.

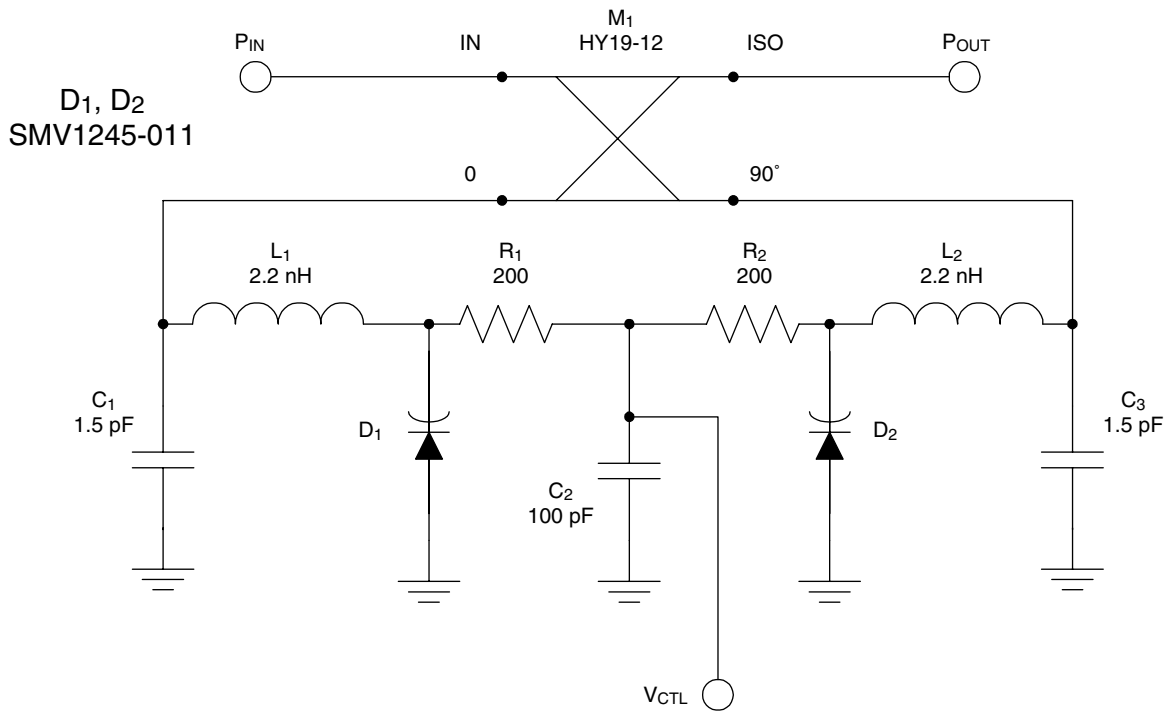


Figure 7. Phase Shifter Circuit Diagram

Designator	Value	Part Number	Footprint	Manufacturer
C ₁	1 pF	CM105CG1R0K10AB	0603	AVX/KYOCERA
C ₂	100 pF	CM105CG200K10AB	0603	AVX/KYOCERA
C ₃	1 pF	CM105CG1R0K10AB	0603	AVX/KYOCERA
M ₁	HY19-12	HY19-12	SOIC-8	Alpha Industries
R ₁	200	CR105-201J-T	0603	AVX
R ₂	200	CR105-201J-T	0603	AVX
D ₁	SMV1245-011	SMV1245-011	SOD-323	Alpha Industries
D ₂	SMV1245-011	SMV1245-011	SOD-323	Alpha Industries
L ₁	2.2 nH	HI1608-1B2N2_N_K_B	0603	ACX
L ₂	2.2 nH	HI1608-1B2N2_N_K_B	0603	ACX

Table 3. Bill of Materials

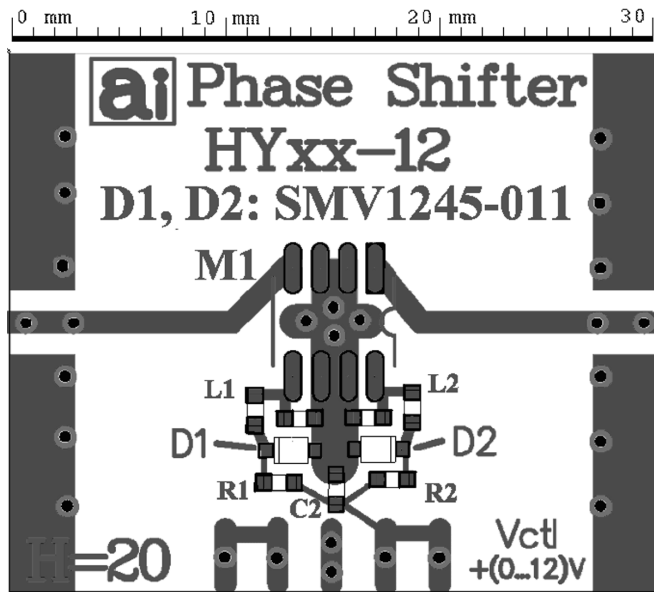


Figure 8. Phase Shifter PCB Layout

Performance Discussion

Measured performance is shown in Figures 9a and 9b with simulated data. Three sets of circuit values were measured and analyzed as shown on the graphs. The largest phase shift, 240°, occurred at $L_{ser} = 2.2$ nH and $C_{par} = 2.0$ pF for varactor voltage change from 0–12 V. In this case, the amplitude variation was about ± 1.5 dB. For $C_{par} = 1.5$ pF there was an approximate 190° phase shift with ± 0.75 dB amplitude variation. With $L_{ser} = 2.2$ nH and $C_{par} = 1.8$ pF there was an approximate 220° phase shift with ± 1.2 dB amplitude variation.

It is interesting to note that the “linear” range of phase shift (linear vs. voltage) is similar for the three designs and is about 120° (from 60° to 180°). The highest phase/voltage sensitivity was for $C_{par} = 2.0$ pF estimated at about 40–50 V. Higher phase shift values are achievable with higher C_{par} values, but larger amplitude variations would occur.

The measured and simulated phase responses were noticeably similar, validating the assumptions in the model that predict phase properties. The simulated amplitude responses were not as close to the measured data. Some of the discrepancies may be attributed to the simplified, idealized model of the 90° hybrid coupler.

In this design, we considered only the SMV1245-011 varactor diode from a large selection of varactors available from Alpha. Varactors with higher tuning sensitivity, such as the SMV1247 or SMV1263, provide a higher range of phase shift but with more amplitude variation. Abrupt junction varactors from the SMV1400 series will operate with lower tuning sensitivity and less phase control but with lower loss and better amplitude linearity.

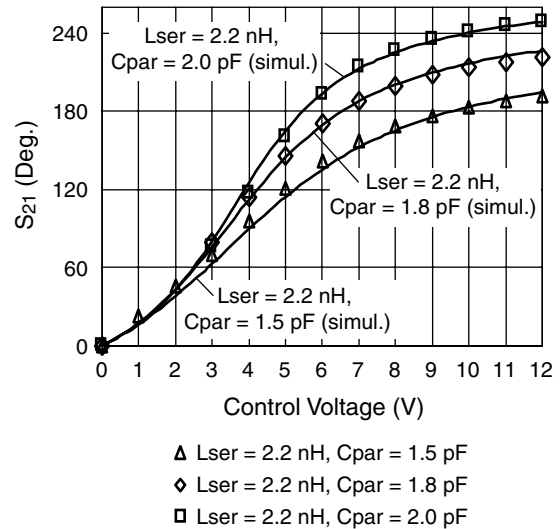


Figure 9a. Phase Response

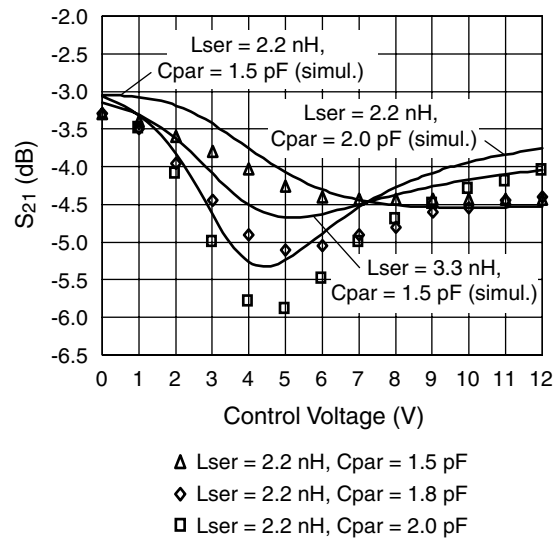


Figure 9b. Amplitude Response

Figure 9a and b. Measured and Simulated Responses of the Phase Shifter

References

1. “Varactor SPICE Models for RF VCO Applications.” APN1004, Alpha Industries, 1998.

List of Available Documents

1. Phase Shifter Simulation Project Files for Libra IV.
2. Phase Shifter PCB Gerber Photo-plot Files.